Available online at www.sciencedirect.com
SCIENCE DIRECT®
Polymer 45 (2004) 1981–1991
polymer
www.elsevier.com/locate/polymer

Comparing the compatibility of various functionalized polypropylenes with thermoplastic polyurethane (TPU)

Qi-Wei Lu[1], Christopher W. Macosko*

Department of Chemical Engineering and Materials Science, University of Minnesota, Minneapolis, MN 55455-0431, USA

Received 29 September 2003; accepted 23 December 2003

Abstract

Three functionalized polypropylenes (PP), a maleated PP (PP-*g*-MA), primary amine functionalized PP (PP-*g*-NH_2), and secondary amine functionalized PP (PP-*g*-NHR), were melt blended with a thermoplastic polyurethane (TPU) at different compositions. Compatibility of each functionalized PP with TPU was compared by investigating the binary blends using rheological (mixer torques, dynamic shear rheometry), thermal (dynamic mechanical analysis), mechanical (tensile test), and morphological (scanning electron microscopy with image analysis, particle size analysis) measurements. Compatibility of the three functionalized PP's with TPU is ranked in a decreasing order as follows: PP-*g*-NHR $\geq$ PP-*g*-NH_2 $\gg$ PP-*g*-MA, which is attributed to higher reactivity of amine (primary and secondary) with urethane linkages. Accordingly, the TPU blends with the two types of amine functionalized PP's exhibited much better synergy, as reflected by much improved mechanical properties including higher tensile strength and ultimate elongation, and finer and more stable morphologies.

Keywords: Reactive compatibilization; Thermoplastic polyurethane (TPU); Amine functionalized polypropylene

1. Introduction

Thermoplastic polyurethane (TPU), with properties covering from a high performance elastomer to tough thermoplastic, has been extensively used due to its superior physical properties (e.g. high tensile strength, abrasion and tear resistance, oil and solvent resistance, low temperature flexibility, paintability, etc.) and high versatility in chemical structures. TPU is a linear segmented block copolymer composed of alternating hard (adduct of diisocyanate and small glycols) and soft (e.g. polyester, polyether, hydrocarbon, silicone, etc.) segments. The hard segments are held together by interchain hydrogen bonds to form physical crosslinks. At melt temperatures, the hydrogen bonds break and linear primary chains are released. Meanwhile, urethane linkages (carbamate, –NHCOO–) in the hard segments become unstable and reversibly decompose into free isocyanate and alcohol [1]. The equilibrium between the urethane linkages and free functional (isocyanate and hydroxyl) groups can be rapidly established [2–4].

Compatibilized blends of TPU and polyolefins (PO) have been investigated for technological, economical, and environmental reasons [5–13]. Anhydride functional PO has been the most frequently used compatibilizer [6,7,11]. While some compatibility with TPU including finer morphology and improved mechanical properties has been reported, no reaction was detected between the functional group and the urethane linkage or free isocyanate group from thermal degradation of TPU. This result is supported by our model study [14]. Reactive compatibilization, i.e. generating graft or block copolymers *in situ* during the process of melt blending, appears to produce the best blend compatibilization [15–18]. However, this requires highly reactive functional groups in order to generate compatibilizers within the typical processing time. In our recent study [14], a series of model urethane reactions showed that amine (both primary and secondary) is the most reactive functional groups toward urethane linkages among commonly used functionalities. In the following work, both primary and secondary amine functional groups were grafted onto polypropylenes (PP) by melt amination [19] and truly

* Corresponding author. Tel.: +1-612-625-6606; fax: +1-612-626-1686.
E-mail address: macosko@umn.edu (C.W. Macosko).
[1] Present address: General Electric Global Research Center, Polymer and Specialty Chemical Technologies, One Research Circle, Niskayuna, NY 12309, USA

0032-3861/$ - see front matter © 2004 Elsevier Ltd. All rights reserved.
doi:10.1016/j.polymer.2003.12.077

compabilized TPU/PP blends were achieved using the amine functionalized PP's (PP-*g*-NH_2 and PP-*g*-NHR) [20].

In this work, compatibility of the PP-*g*-NH_2 and PP-*g*-NHR with TPU was studied and compared with that of a maleated PP (PP-*g*-MA). The compatibility was investigated with rheological (mixer torques, dynamic shear rheometry), morphological (scanning electron microscopy with image analysis, particle analysis), thermal (dynamic mechanical analysis), and mechanical (tensile test) measurements.

2. Experimental

2.1. Materials

The thermoplastic polyurethane (TPU, Avalon 70AE, Shore hardness: 70A) was provided by Huntsman. The PP-*g*-MA (Fusabond P MZ-109D; MFI = 120 g 10 min^{-1}, ASTM D1238; M_w = 30.7 kg mol^{-1}, PDI = 2.9) was obtained from DuPont. The anhydride graft content is 0.55 wt% according to the supplier. The PP-*g*-NH_2 (PP-*g*-MA/hexamethylenediamine, 1:1.5 by molar ratio of MA to diamine) and PP-*g*-NHR (PP-*g*-MA/N-hexylethylenediamine, 1:1 by molar ratio of MA to diamine) were prepared according to the method reported previously [19]. All the raw materials were dried at 80 °C in a vacuum oven overnight before processing.

2.2. Melt blending

Pellets of TPU and each of the functionalized PP's (PP-*g*-X, X = MA, NH_2, or NHR) at different weight ratios (TPU to PP in this paper) were blended on an instrumented batch mixer (HBI System 90, Haake) with two counter-rotating roller blades at 190 °C and 75 rpm for 5 min.

2.3. Rheology

The rheological behaviors were measured at 190 °C on a dynamic stress rheometer (SR-200, Rheometric Scientific) with a 25-mm parallel-plate and 1-mm gap over a frequency range of 500–0.1 rad s^{-1}. Samples were compression-molded (Wabash compression molder) at 185 °C under a pressure of 0.55 MPa for 10 min to 25 mm round disks.

2.4. Gel permeation chromatography

Each of the TPU/PP-*g*-X (X = MA, NH_2, or NHR) (90/10 and 70/30) blends was immersed in tetrahydrofuran (THF). TPU was extracted and the insoluble PP phase was filtered out. TPU molecular weight and distribution was determined by gel permeation chromatography (GPC). Each sample (~1.0 mg ml^{-1}) was run at room temperature in THF as a carrier solvent with a flow rate of 1.0 ml min^{-1} (Waters 717 plus an autosampler). Two detectors were used, including an internal differential refractive index detector and an external ultraviolet detector. The column used was Jordi Gel DVB Mixed Bed, which was calibrated with poly(styrene) standards (EasiCal PS-2, Polymer Laboratories) of 10 known molecular weights. One drop of phenyl isocyanate was added into the samples that may contain free amine groups before loading to prevent adsorption of the amine to the column.

2.5. Scanning electron microscopy and image analysis

TPU/PP-*g*-X (X = MA, NH_2, or NHR) (90/10 and 30/70) blends were cryo-fractured in liquid nitrogen and stained in RuO_4 vapor for 20 min. The fracture surface was coated with platinum of 10 Å for examination of morphology by scanning electron microscopy (S-900, Hitachi) with an accelerating voltage of 10 kV. Both secondary electron images for topology and backscattered electron images for phase contrast were taken. The interfacial area per unit volume was estimated from backscattered micrographs using a 2D digital image processing method [21], which calculates interface perimeter/area from the number of pixels along the interface.

2.6. Particle analysis

Each of the blends containing 90 wt% TPU was immersed in THF to dissolve the TPU matrix and obtain a fine dispersion of PP particles. PP particle size and distribution was measured at room temperature on a particle analyzer (LS230, Coulter). The measurements were repeated after the samples were annealed at 190 °C for 30 min.

2.7. Dynamic mechanical analysis

Rectangular specimen (10 mm × 2 mm × 0.8 mm) of the 70/30 blends were prepared by the same compression molding method. Each sample in nitrogen atmosphere was loaded with extensional force at a sine wave frequency of 1.0 Hz (DMA 7e, Perkins–Elmer). The temperature was scanned from −60 °C to soft temperatures at a heating rate of 5 °C/min. The initial strain level is approximately 0.4%.

2.8. Tensile test

Dumbbell specimens (ASTM D638, type IV) were also prepared by compression molding. Tensile tests (Universal Tester Model 5500, Instron) of the TPU/PP-*g*-X (X = MA, NH_2, or NHR) blends were performed at room temperature with a loading speed of 50 mm/min.

3. Results and discussion

3.1. Rheology

Steady-state torques (values at 5 min) during the melt blending of the TPU and functionalized PP's in the batch mixer versus blend composition are plotted in Fig. 1. Note that there is a significant torque maximum at 50–90% PP-*g*-NH_2, while the blends with other two functionalized PP's have lower torques than the non-functional PP blends.

Blend viscosities (η) can be converted from torque (i.e. stress) and rotor speed (i.e. shear rate) through a model proposed by Lee and Purdon [22]. The viscosity at 75 rpm is estimated as [23]:

$$\eta = \frac{4.59n(1 - 0.924^{2/n})M}{a}(\text{Pa s}) \quad (1)$$

where M = torque, m-gf, n = power law index, a = instrumental constant.

The instrumental constant, a, is a material specific parameter. As discussed previously [23], a proper instrumental calibrations cannot be done for TPU because it is uncertain how this constant will change with the molecular weight of the material. While it is difficult to calculate real viscosities from the mixer torque, the batch mixing torques can still be qualitatively compared with the data from rheological measurements.

Dynamic shear rheometry enables us to better understand the rheological behavior of the binary blends. The complex viscosities and storage moduli of the TPU/PP-*g*-X (X = MA, NH_2, or NHR) blends at some compositions are shown in Fig. 2(a) and (b), respectively. Viscosity of TPU is close to that of PP-*g*-NH_2, which is higher than that of PP-*g*-MA and PP-*g*-NHR. The 90/10 and 10/90 compositions are of most interest because both morphologies are simply droplets of one phase dispersed in a matrix of the other. The viscosity of TPU/PP-*g*-X (X = MA, NH_2, or NHR) at 90/10 can be ranked as follows: TPU/PP-*g*-MA > TPU/PP-*g*-NH_2 > TPU > TPU/PP-*g*-NHR; while that at 10/90: TPU/PP-*g*-NH_2 ≫ TPU ≫ TPU/PP-*g*-NHR > TPU/PP-*g*-MA. The TPU/PP-*g*-NH_2 blend at 10/90 exhibits a gel-like structure and its storage modulus has a slope of approaching zero at low frequency (0.1 rad s^{-1}) in the log–log scale plot.

Since the maximum shear rate in the chamber of the batch mixer at 75 rpm was estimated to be 71 s^{-1} [23], the values of complex viscosities and storage moduli plotted in Fig. 3 were taken at the closest data point, 79 rad s^{-1}. Although viscosities from the mixer torques cannot be easily obtained, the blend viscosities (Fig. 3(a)) and storage moduli (Fig. 3(b)) show similar trends with change of composition, consistent with the torque values in Fig. 1. There is a compositional window for each type of blend where the viscosity turns out to be higher than the neighboring compositions. Higher viscosities compared with either pure component may be desirable in melt processing, e.g. extrusion and blow molding with less sagging. It occurs around 10 wt% for PP-*g*-MA, 30 wt% for PP-*g*-NHR, and 70–90 wt% for PP-*g*-NH_2. It is indicative of formation of either a physical or chemical network, or at least strong interfacial interactions between the two different phases. Because viscosity of uncompatibilized blend usually becomes lower in the co-continuity region. Torques of blending TPU and a non-functional PP (PP13M11, Huntsman) were also shown in Fig. 1 as an example. At around 50/50, the blend viscosity becomes lowest and even lower than that of either homopolymer. Since there is very weak interaction (van der Waals force) and high interfacial tension between the TPU and PP, the lower viscosity is probably due to an interfacial slip between the uncompatibilized phases [24].

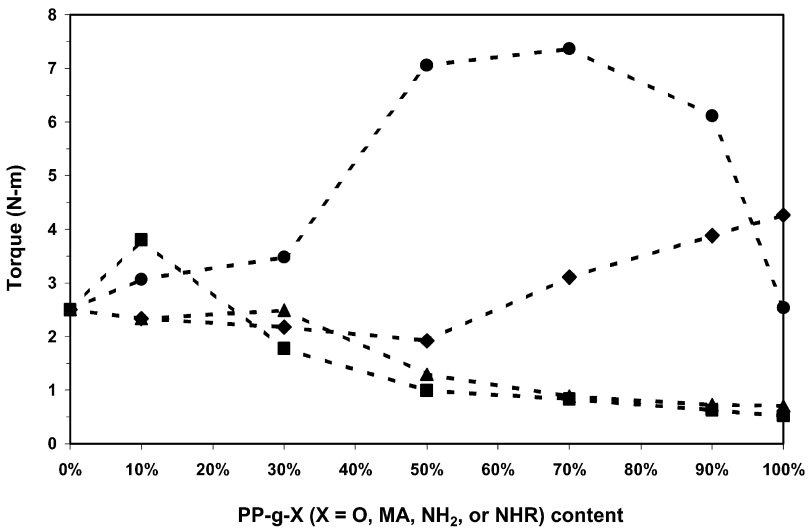

Fig. 1. Torques of blending for TPU/PP-*g*-X (X = non, ◆; MA, ■; NH_2, ●; NHR, ▲) at different compositions.

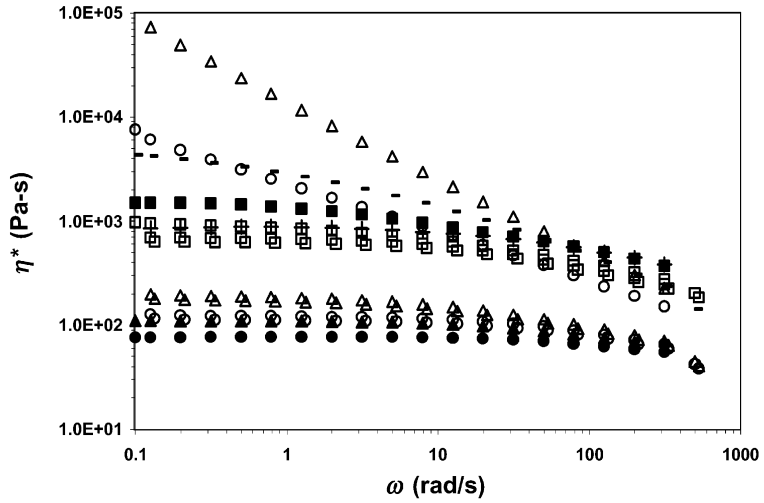

(a)

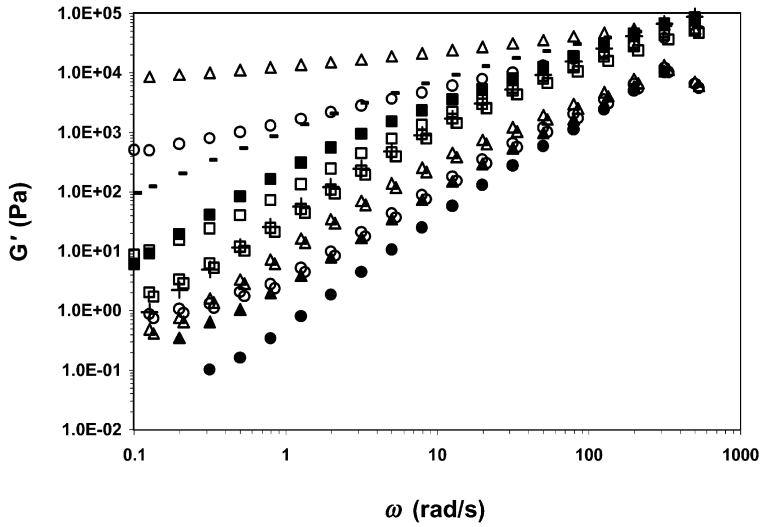

(b)

Fig. 2. (a) Complex viscosity (η^*) and (b) storage modulus (G') as a function of dynamic frequency (ω) for the TPU/PP-*g*-X (X = MA, NH_2, or NHR) blends at different compositions: TPU (+); 90/10: TPU/PP-*g*-MA (■), TPU/PP-*g*-NH_2 (□), TPU/PP-*g*-NHR (shadowed □); 10/90: TPU/PP-*g*-MA (▲), TPU/PP-*g*-NH_2 (▲), TPU/PP-*g*-NHR (shadowed △); 0/100: PP-*g*-MA (●), PP-*g*-NH_2 (○); PP-*g*-NHR (shadowed ○); PP (—).

3.2. GPC

It is always desirable to detect whether compatibilizers are formed and, if possible, how much are formed. While GPC is a frequently used method, it is difficult in TPU/PP due to: (1) insolubility of PP at room temperature; (2) no mutual solvent for TPU and PP even at elevated temperature; (3) broad molecular weight distributions of both TPU and PP; (4) TPU molecular weight reduction due to thermal degradation [23]. We were only able to measure molecular weight changes in the TPU component. From these we attempt to estimate the grafting of TPU to PP-*g*-X. Only 90/10 and 70/30 blends were examined where the TPU phase is continuous and limited amount of TPU inclusion in PP was found so that it can be most extracted out by THF.

It is known that the urethane linkage is unstable and prone to dissociation at melt processing temperatures. Although this process is reversible, TPU molecular weight decreases after processing due to the effects such as fast cooling, moisture, mechanical degradation, etc. After mixing pure TPU under the same conditions, molecular weight dropped ~20% (see Table 1). After blending with the functionalized PP's, molecular weight is expected to further decrease, which is clearly seen in Table 1. The more functionalized PP added, the lower the molecular weight of the TPU product. In the three types of blends TPU molecular weight decreases as follows: TPU/PP-*g*-MA > TPU/PP-*g*-NH_2 > TPU/PP-*g*-NHR. The TPU/X (X = MA, NH_2, or NHR) molar ratio is estimated to be 1.7 for a 90/10 blend and 0.4 for a 70/30 blend, according to

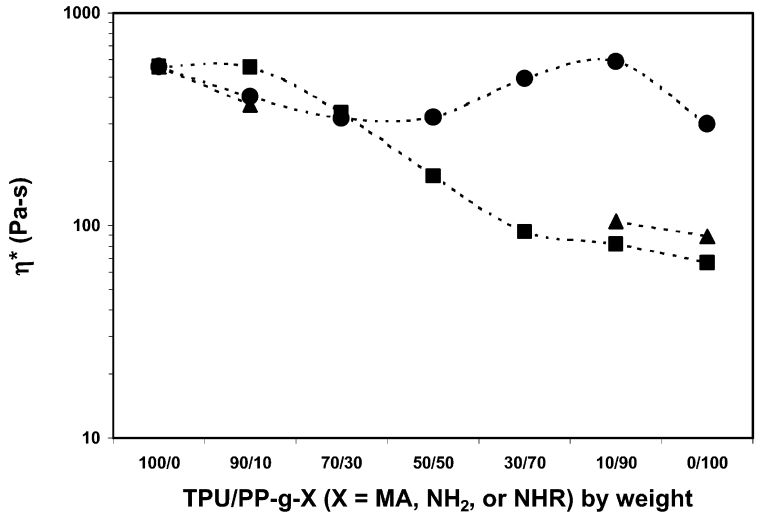

(a)

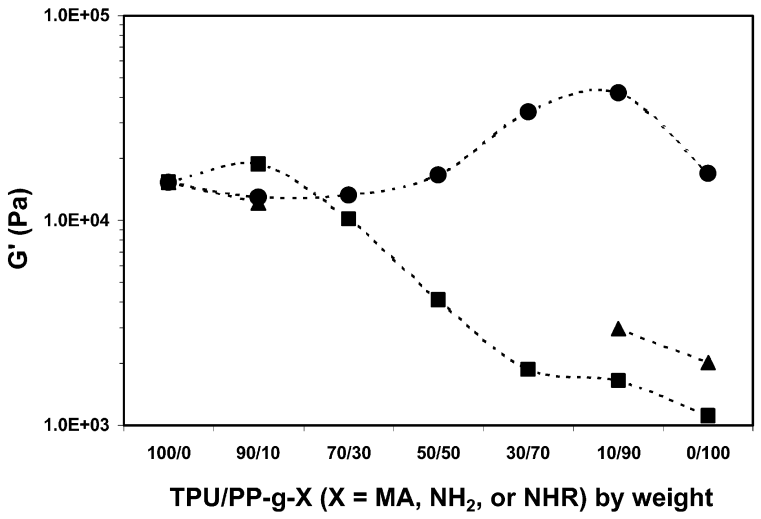

(b)

Fig. 3. (a) Complex viscosity (η^*) at 79 rad s^{-1} and (b) storage modulus (G') at 79 rad s^{-1} of the TPU/PP-*g*-X (X = MA, ■; NH_2, ●; NHR, ▲) blends at different compositions.

TPU molecular weight and graft content of PP-*g*-MA. It should be noted that the numbers may be considerably higher because real TPU molecular weights are usually lower than the values based on polystyrene standards [25].

If a molar fraction, x, of total TPU molecules with initial molecular weight M_i react with PP-*g*-X, the TPU molecular weight (M_t) in the blend product will be:

$$M_t = (1-x)M_i + x\frac{M_i}{2} \Rightarrow x = 2\left(1 - \frac{M_t}{M_i}\right) \quad (2)$$

Table 1
Number and weight average molecular weight (M_n and M_w, respectively) and polydispersity index (PDI) of TPU before and after blending with PP-*g*-X (X = MA, NH_2, or NHR)

	TPU		TPU/PP-*g*-MA		TPU/PP-*g*-NH_2		TPU/PP-*g*-NHR	
	Raw	As extruded	90/10	70/30	90/10	70/30	90/10	70/30
M_n (kg/mol)	96	78	75	64	75	62	65	60
M_w (kg/mol)	174	134	129	112	129	103	115	98
PDI	1.82	1.73	1.72	1.74	1.73	1.66	1.76	1.65
TPU conversion	–	–	7.7%	36%	7.7%	41%	33%	46%

This relation assumes that a random scission of the TPU chains results in a half of the starting molecular weight and the copolymers generated by the interfacial reactions remain in the PP phase. To remove the effect of simple thermal degradation on TPU molecular weight, M_i is taken to be 78 kg/mol. The conversion of TPU molecules can thus be calculated (see Table 1).

The reaction of PP-*g*-NHR with TPU is obvious and the TPU conversion is high in both 90/10 and 70/30 blends. While the high conversion is not seen in TPU/PP-*g*-MA (90/10) and TPU/PP-*g*-NH_2 (90/10), it is found in TPU/PP-*g*-MA (70/30) and TPU/PP-*g*-NH_2 (70/30). This contradicts our results using model urethanes [14] which predict that the anhydride should not react with TPU. Given these results and the difficulties discussed above, we conclude that GPC fails to provide a clear evidence of the copolymer formation. The reactions or interactions between the TPU and functionalized PP's have to be investigated by more indirect methods.

3.3. Morphology

Blend morphology exhibiting both quality and quantity of interface is usually indicative of the existence and effect of compatibilizers, i.e. copolymers in this case. Scanning electron microscopy (SEM) is a powerful tool to examine morphology in polymer blends. Secondary electron images (SEI) and backscattered electron images (BEI) provide different information. SEI displays topology and BSI shows contrasted phases. BEI enables us to clearly see the features even when they are hiding below the surface. In practice, secondary electron detector can receive some secondary electrons and vice versa. Nonetheless good staining is necessary and crucial. RuO_4 was used because only TPU contains unsaturated phenyl rings which can be selectively stained. The stained TPU phase containing the heavy metal atoms is able to scatter back more electrons and thus looks much brighter in the SEM images.

Two compositions for each of the TPU/PP-*g*-X (X = MA, NH_2, or NHR) blends are illustrated: 30/70 in Fig. 4 and 90/10 in Fig. 5. Both figures show morphology of particles of one component dispersed in the matrix of the other. Domain size and interfacial adhesion are the two important aspects. Compared with the TPU/PP-*g*-MA blends, TPU/PP-*g*-NH_2 or THP/PP-*g*-NHR blends display significantly finer morphology, i.e. much reduced particle size of the dispersed phase. In addition, particle size distributions are narrower. These reflect a lower interfacial energy due to the compatibilizers generated by the fast interfacial reactions between amine and urethane linkages. The interfaces in the TPU/PP-*g*-MA blends are much weaker and lack of sufficient adhesion. Some TPU particles were pulled out from the matrix during the cryo-fracturing, which was not observed in the blends of amine functionalized PP's. The stronger interface is also indicative of copolymer formation at the interface because the copolymers can 'stitch' the two phases together. The effect was clearly seen in the strikingly higher adhesion between TPU and amine functionalized PP's that was quantified by double cantilever beam test [26].

3.4. Particle size

To compare the differences in particle size and distribution quantitatively, the TPU matrix in the TPU/PP-*g*-X (90/10) blends was dissolved in THF to form a fine dispersion of PP particles. The particle size distributions of the functionalized PP's are plotted in Fig. 6. The amine functionalized PP's show significantly reduced sizes, shifting to the sub-micron range. Details about the structures of the amine functionalized PP's can be ascertained from the curves. PP-*g*-NHR displayed two peaks including a very tiny one with larger size, which is probably due to a small percentage ($\sim$6%) of uncapped PP-*g*-MA after melt amination. Three peaks were seen for PP-*g*-NH_2. The one with a size even larger than that of PP-*g*-MA is most likely due to the branching or microgels formed during the melt amination process [19]. Table 2 lists the volume and surface area average diameters (D_v and D_s, respectively). The particle size is ranked in a decreasing order: PP-*g*-MA > PP-*g*-NH_2 > PP-*g*-NHR. So does the size distribution that is characterized as D_v/D_s. The PP-*g*-NHR particles exhibit a significantly narrow distribution with $D_v/D_s = 1.1$.

After annealing, the PP-*g*-MA and PP-*g*-NH_2 particles nearly doubled their sizes (cf. Table 2) due to coalescence. In contrast, the PP-*g*-NHR particles kept the small size and narrow size distribution, displaying excellent morphology stability against annealing due to the 'steric effect' of the compatibilizers at the interface that inhibit the coalescence [27].

The domain size can also be roughly estimated from the amount of interface per unit area by image analysis of the scanning electron micrographs. In principle, the image analysis works for any composition, e.g. 30/70 (TPU/PP-*g*-X) that is inaccessible to the light scatting that requires a liquid medium. The amount of interface per unit area (i.e.

Table 2
Average particle size of 10 wt% PP-*g*-X (X = MA, NH_2, or NHR) in TPU blends by light scattering and image analysis

Particle size (μm)	TPU/PP-*g*-MA		TPU/PP-*g*-NH_2		TPU/PP-*g*-NHR	
	90/10	30/70	90/10	30/70	90/10	30/70
D (by SEM)	0.60	5.10	0.50	2.48	0.32	2.49
D_s[a]	0.64	–	0.46	–	0.31	–
D_s (after annealing)	1.24	–	0.92	–	0.29	–
D_v[b]	1.30	–	0.82	–	0.34	–
D_v/D_s	2.0	–	1.8	–	1.1	–

[a] Note: D_s = surface area average diameter, $\propto \sum D^3/\sum D^2$.
[b] D_v = volume average diameter, $\propto \sum D^4/\sum D^3$.

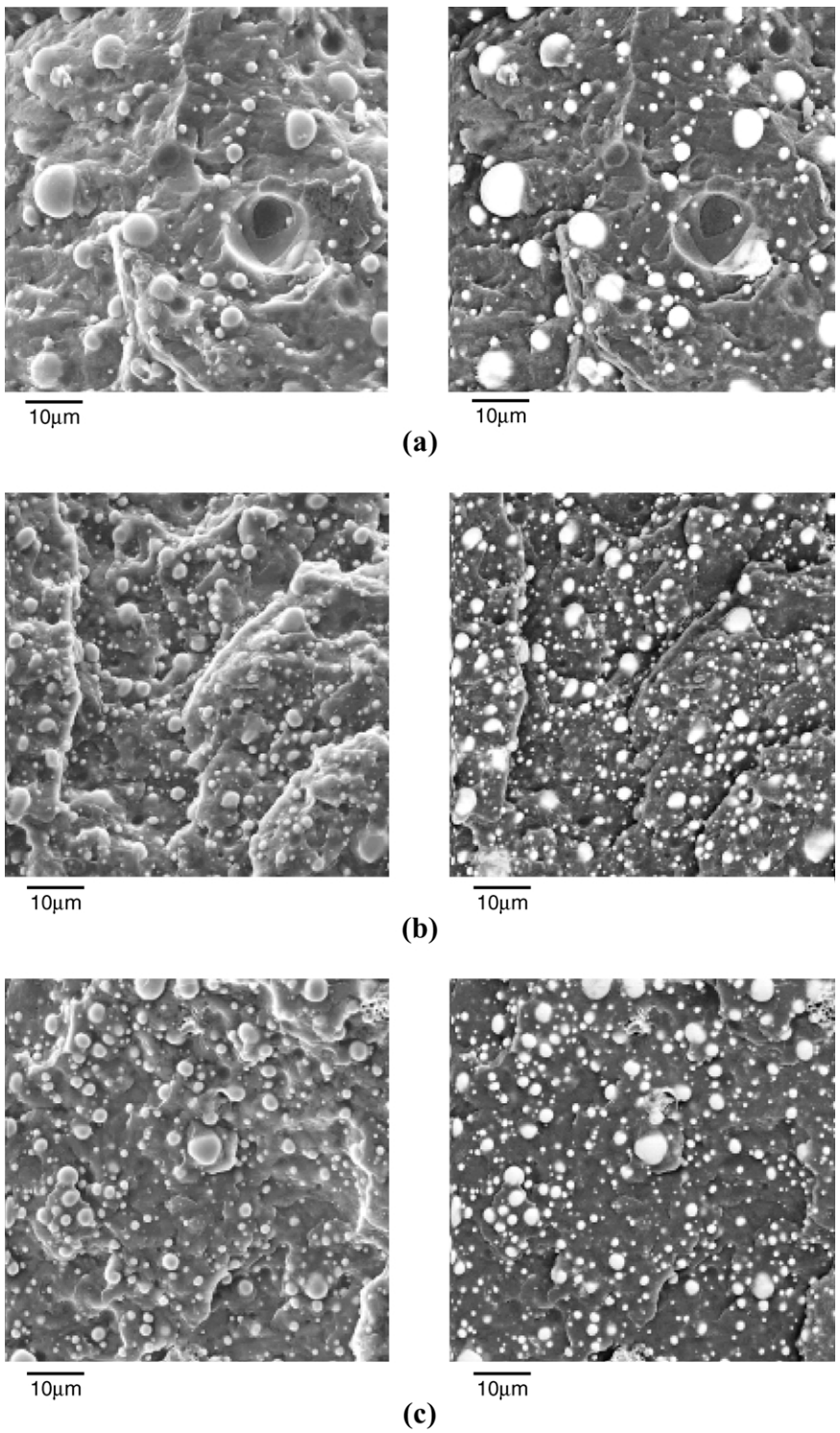

Fig. 4. Scanning electron micrographs of the TPU/PP-*g*-X (X = MA, NH_2, or NHR) blends (30/70 by weight). Both secondary electron image for topology (left) and backscattered electron image for phase contrast (right; note: TPU, white; PP, black) are presented. (a) X = MA; (b) X = NH_2; (c) X = NHR.

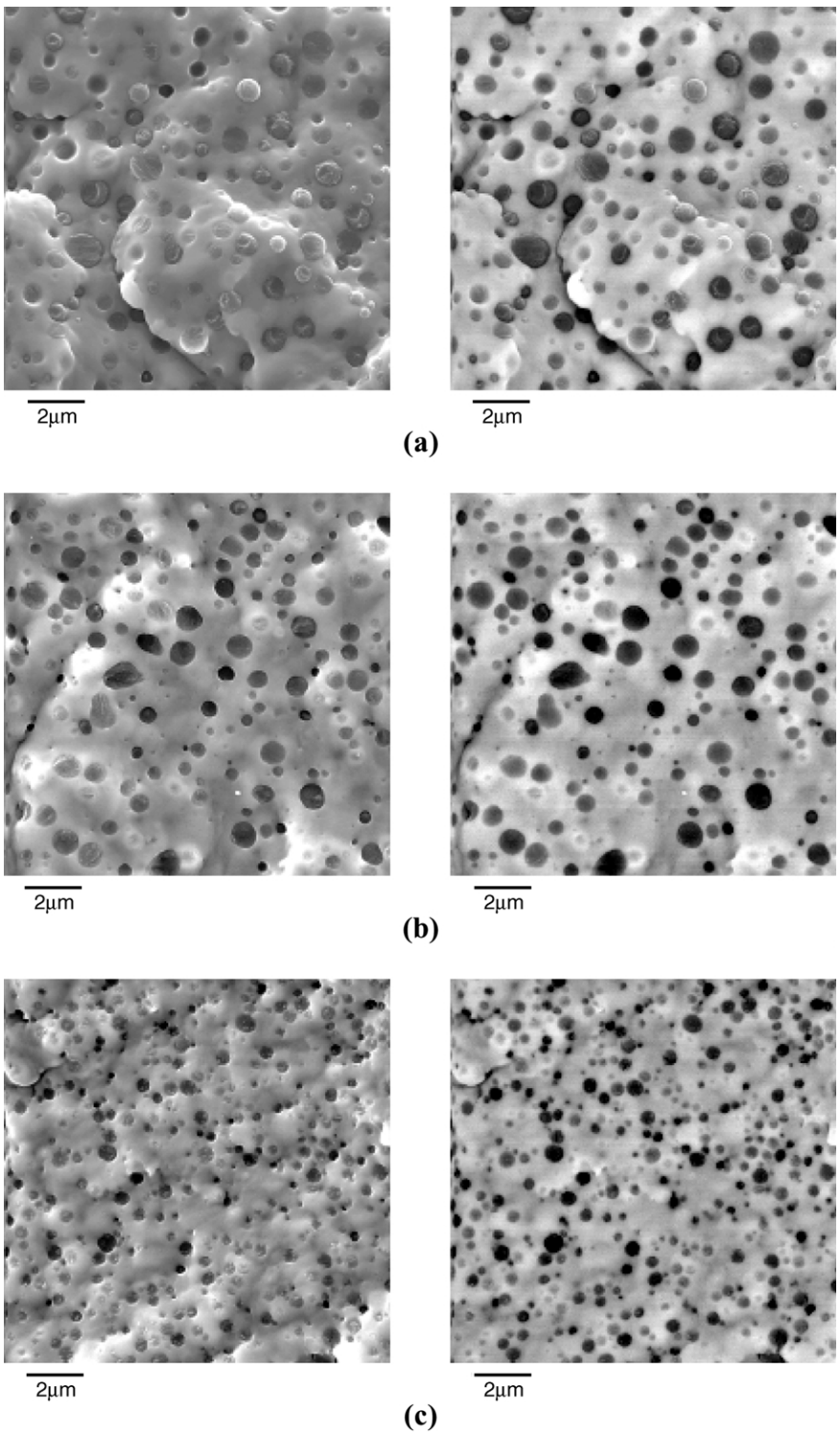

Fig. 5. Scanning electron micrographs of the TPU/PP-*g*-X (X = MA, NH_2, or NHR) blends (90/10 by weight). Both secondary electron image for topology (left) and backscattered electron image for phase contrast (right; note: TPU, white; PP, black) are presented. (a) X = MA; (b) X = NH_2; (c) X = NHR.

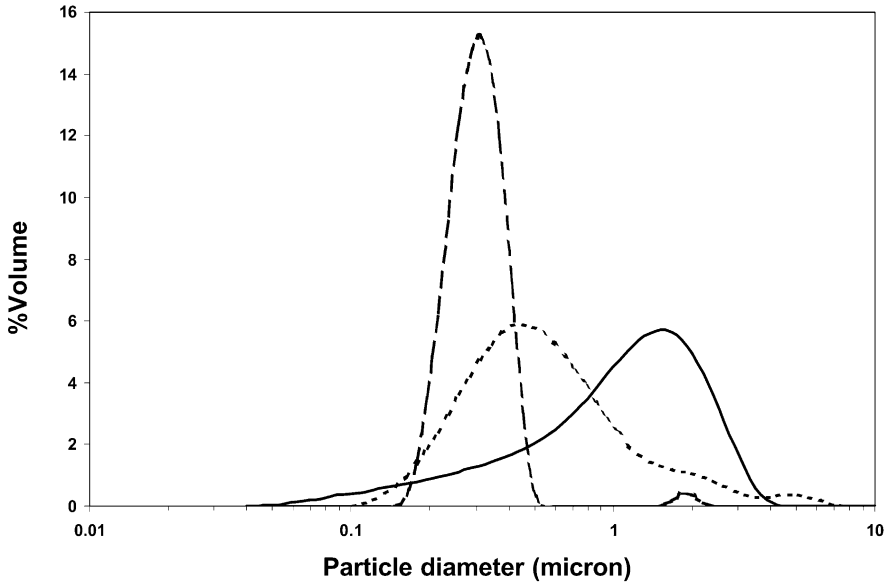

Fig. 6. Particle size distributions of 10 wt% PP-*g*-X (X = MA, —; NH_2, - - - -; NHR, – –) in TPU blends. The curves are normalized.

interfacial area per unit volume for a random cut), *AI*, can be approximately correlated to the average particle size (*D*) through following relationship:

$$AI = \frac{n\pi D}{A} = \frac{n\pi D}{n\pi\left(\frac{D}{2}\right)^2 / \left(\frac{6^{2/3}\pi^{1/3}}{4}\Phi^{2/3}\right)}$$

$$= \frac{4.84\Phi^{2/3}}{D} \propto \frac{1}{D} \quad (3)$$

where n = number of particle/area, A = image area of analysis, Φ = volume fraction of the dispersed phase.

The values of particle size from image analysis of SEM micrographs and from particle size analysis by light scattering agree very well (cf. Table 2). Both amine functionalized PP's blends have more than doubled amount of interface, indicating much reduced interfacial tension between TPU and the amine functionalized PP phases. To summarize the morphological study, the compatibility of the three functionalized PP's with TPU is ranked as follows: PP-*g*-NHR > PP-*g*-NH_2 > PP-*g*-MA.

3.5. Mechanical properties

Elastic or storage moduli (E') of TPU blends with each of PP-*g*-X (X = MA, NH_2, or NHR) as well as with the non-functional PP at 70/30 are plotted as a function of temperature in Fig. 7. Over the temperature range E' ranks in a decreasing order as follows: TPU/PP-*g*-NHR > TPU/PP-*g*-NH_2 > TPU/PP-*g*-MA > TPU/PP, which agrees with the morphology results. The TPU in this work is an elastomeric material with a tensile modulus of only 6.7 MPa, The modulus of TPU blends depends on both quantity and quality of the interface between TPU and PP. The volume fraction of the interfacial region can be estimated as $\frac{6\Phi h}{D} \sim \frac{h}{D}$,, where Φ and D are defined above and h is the thickness of interface, typically 1–10 nm. Interfacial compatibilizers can result in finer dispersion (see Table 2) and broader interfaces, leading to a much higher interfacial region content. They can also produce stronger interfaces that are responsible for more efficient stress transfer across interface. The E' values at room temperature (25 °C) are listed in Table 3. The modulus is more than doubled from TPU/PP-*g*-MA to TPU/PP-*g*-NH_2, as well as from TPU/PP-*g*-NH_2 to TPU/PP-*g*-NHR.

Stress–strain curves of TPU/PP-*g*-X (X = MA, NH_2, or NHR) blends at three different compositions (30/70, 50/50, and 70/30) are plotted in Fig. 8. The values of tensile modulus, strength, and ultimate elongation are listed in Table 3. The TPU is a soft elastomer and functionalized PP's are rigid plastics, representing two extreme tensile behaviors. In blends, the TPU phase contributes to

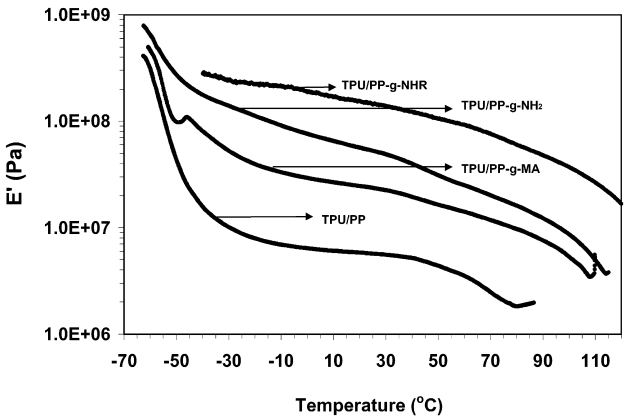

Fig. 7. Extensional storage modulus (E') as a function of temperature for the TPU/PP and TPU/PP-*g*-X (X = MA, NH_2, or NHR) blends with 70 wt% TPU.

Table 3
Mechanical properties of TPU/PP-*g*-X (X = MA, NH_2, or NHR) blends

	TPU/PP-*g*-MA			TPU/PP-*g*-NH_2			TPU/PP-*g*-NHR		
	70/30	50/50	30/70	70/30	50/50	30/70	70/30	50/50	30/70
E' (MPa)	23.6	–	–	52.6	–	–	145	–	–
Elastic modulus (MPa)	15.5	239	475	44.3	205	515	141	305	600
Tensile strength (MPa)	6.35	14.4	21.6	14.1	14.0	23.8	22.3	14.1	22.0
Ultimate elongation (%)	–	129	13.3	–	525	43.6	–	1165	33.4

elongation and can toughen the PP matrix; while, conversely, the functionalized PP's contribute to strength and modulus, reinforcing the TPU matrix. If the blends are well compatibilized, good synergies between elongation and strength will be achieved. When TPU is a major phase as TPU composition ≥ 70 wt%, a slip between the specimen and grip occurred at very high strain levels ($>1200\%$) and the specimens could not be broken. The ultimate elongations for these samples were thus unavailable. It is noted that the tensile moduli of the 70/30 blends and storage moduli from the dynamic mechanical analysis are consistent and have the same ranking: TPU/PP-*g*-NHR > TPU/PP-*g*-NH_2 > TPU/PP-*g*-MA. The tensile behaviors of two amine functionalized PP blends are very close to each other and their strengths nearly double that of the PP-*g*-MA one.

The TPU blends at 50/50 are cocontinuous. From the tensile curves in Fig. 8, one can easily tell how strong the interface is to effectively transfer the stress especially at large stress and strain. The two amine functionalized PP blends display much larger ultimate elongations than the PP-*g*-MA one. TPU/PP-*g*-NHR at 50/50 exhibits an even much larger elongation at break than TPU/PP-*g*-NH_2 at 50/50. As 30 wt%, where TPU turns to be a minor phase in the PP-*g*-X (X = MA, NH_2, or NHR) matrix, the enhanced tensile properties are still quite obvious for the blends of two amine functionalized PP's compared with the blend of PP-*g*-MA.

Overall, the two amine functionalized PP's have significantly higher compatibility with TPU than the PP-*g*-MA, leading to larger interfacial area, stronger interface, higher morphology stability, and accordingly much better synergies in blends. The PP-*g*-NHR has slightly better effect than the PP-*g*-NH_2. Accordingly, compatibility of the three functionalized PP's with TPU can be ranked in a decreasing order as follows: PP-*g*-NHR $\geq$ PP-*g*-NH_2 $\gg$ PP-*g*-MA. The significantly greater compatibility of the two amine functionalized PP's was due to the much higher reactivity of amine (primary and secondary) functional groups with urethane linkages. The higher reactivity of the functionalized PP leads to more compatibilizers (i.e. block or graft copolymers) generated during the melt blending and eventually results in better material properties. Noting that the functionalized PP's were used without dilution in this work, we should see more dramatic improvement of the compatibility effectiveness in practical applications of polymer blends [20].

The compatibility ranking contradicts the reactivity order: primary amine > secondary amine $\gg$ anhydride [14]. It is actually the quality of the PP-*g*-NH_2 from the melt amination process [19] that impedes its effectiveness in

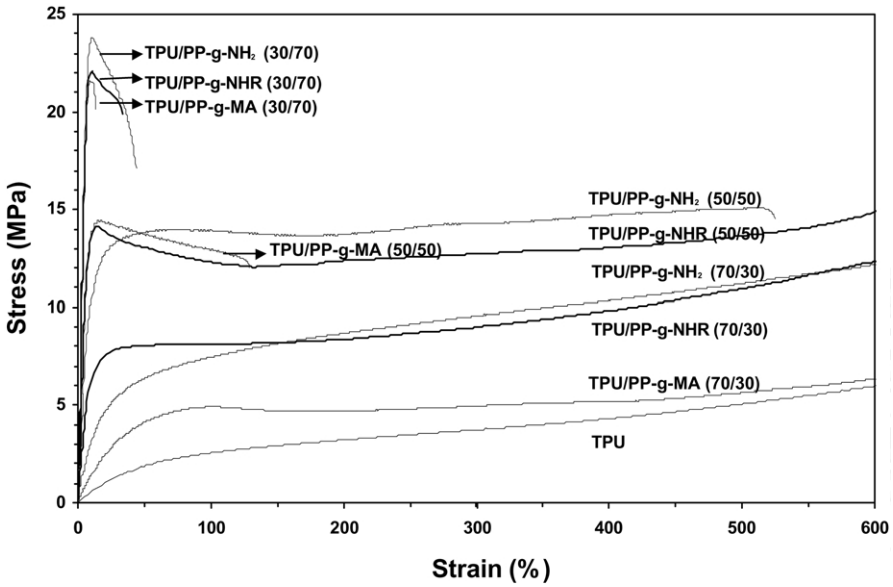

Fig. 8. Stress–strain curves of the TPU/PP-*g*-X (X = MA, NH_2, or NHR) blends.

the blends with TPU. There is residual primary–primary diamine (hexamethylene diamine) left in the product even after being vacuum-heated in post-processing. The small molecule may primarily react with urethane linkages due to its greater mobility, which interferes with the reaction of the amine groups grafted on the PP chains with urethane linkages. It causes less copolymers to be formed by the PP-*g*-NH_2 even though it has higher reactivity. Meanwhile, both primary and secondary amine groups are reactive enough with urethane linkages to form compatibilizers under the melt blending conditions (200 °C, 5 min) [14]. Therefore, the PP-*g*-NHR shows slightly higher compatibility with TPU than the PP-*g*-NH_2. The authors believe that the PP-*g*-NH_2 will show higher compatibility if a better (unquestionably challenging) way of its preparation is invented.

4. Conclusions

Compatibility of the three functionalized PP's with TPU is ranked in a decreasing order as follows: PP-*g*-NHR $\geq$ PP-*g*-NH_2 $\gg$ PP-*g*-MA, which was confirmed rheologically, morphologically, and mechanically. Inferior quality of the PP-*g*-NH_2 to that of the PP-*g*-NHR due to the melt amination process results in less compatibilizer formation even though its higher reactivity.

Acknowledgements

The authors thank Troy Peterson for help with sample preparations and some experiments. Helpful discussions with Dr Jacques Horrion were highly appreciated. This work was funded by Huntsman Polyurethanes, an international business of Huntsman International LLC.

References

[1] Bayer O. Diisocyanat-polyadditions. München: Carl Hanser; 1963.
[2] Kawakami Y, Murthy RAN, Yamashita Y. Polym J 1981;13:343–9.
[3] Yang WP, Macosko CW, Wellinghoff ST. Polymer 1986;27:1235–40.
[4] Joel D, Hauser A. Die Makromol Chem 1994;217:191–9.
[5] Zabrocki VS. European Patent No. 347794; 1989.
[6] Tang T, Jing X, Huang B. J Makromol Sci—Phys 1994;B33:287.
[7] Stutz H, Pötschke P, Mierau U. Macromol Symp 1996;112:151.
[8] Wallheinke K, Pötschke P, Stutz H. J Appl Polym Sci 1997;65:2217.
[9] Papadopoulou CP, Kalfoglou NK. Polymer 1998;26:7015.
[10] Papadopoulou CP, Kalfoglou NK. Polymer 1999;40:905.
[11] Wallheinke K, Pötschke P, Macosko CW, Stutz H. Polym Engng Sci 1999;39:1022.
[12] Ciebien JF, Archey RL, Noble HL. US Patent No. 6174959; 2001.
[13] Farah H, Lerma F, Jr. US Patent No. 6469099; 2002.
[14] Lu Q-W, Hoye TR, Macosko CW. J Polym Sci: Part A: Polym Chem 2002;40:2310.
[15] Ajji A, Utracki LA. Polym Engng Sci 1996;36:1574.
[16] Koning C, Van Duin M, Pagnoulle C, Jerome R. Prog Polym Sci 1998;23:707.
[17] Majumdar B, Paul DR. In: Paul DR, Bucknall CB, editors. Formulation. Polymer blends, vol. 1. New York: Academic; 2000. p. 540–1. Chapter 17.
[18] Macosko CW, Jeon HK, Schulze JS. In: Buschow KHJ, Cahn RW, Flemings MC, Illschner B, Kramer EJ, Mahajan S, editors. Encyclopedia of materials: science and technology, vol. 1. Oxford: Elsevier; 2002. p. 683–8.
[19] Lu Q-W, Macosko CW, Horrion J. Submitted for publication. Lu Q-W. PhD Thesis, Dept. of Chem. Eng. and Materials Sci., U. of Minnesota. 2003.
[20] Lu Q-W, Macosko CW, Horrion J. Macromol Symp 2003;198:221.
[21] Galloway JA, Montminy MD, Macosko CW. Polymer 2002;43:4715.
[22] Lee GCN, Purdon JR. Polym Engng Sci 1969;9:360.
[23] Lu Q-W, Hernandez-Hernandez ME, Macosko CW. Polymer 2003;44:3305.
[24] Zhao R, Macosko CW. J Rheol 2002;46:145.
[25] Hernandez-Hernandez ME. PhD Thesis, Depart. of Chem. Eng. and Materials Sci., U. of Minnesota; 1994.
[26] Lu Q-W, Macosko CW. Polym Prepr ACS Div PMSE 2003;89:844.
[27] Lyu S-P, Jones TD, Bates FS, Macosko CW. Macromolecules 2002;35:7845. Lyu S.-P. Macromolecules 2003;36:10052